PROCEEDINGS OF SCIENCE

Measurement of $\phi_s^{J/\psi\phi}$ at DØ

A. Chandra[*†]
Rice University
E-mail: avdhesh@fnal.gov

This paper is a review of measurement of the *CP*-violating phase $\phi_s^{J/\psi\phi}$ and the decay width difference for the two mass eigenstates $\Delta\Gamma_s$ from flavor-tagged decay $B_s^0 \to J/\psi\phi$: $\Delta\Gamma_s = 0.19 \pm 0.07\,(\text{stat})\,^{+0.02}_{-0.01}\,(\text{syst})\ \text{ps}^{-1}$, $\phi_s^{J/\psi\phi} = -0.57^{+0.24}_{-0.30}\,(\text{stat})\,^{+0.07}_{-0.02}\,(\text{syst})$. The allowed 90% C.L. intervals of $\Delta\Gamma_s$ and ϕ_s are $0.06 < \Delta\Gamma_s < 0.30\ \text{ps}^{-1}$ and $-1.20 < \phi_s < 0.06$, respectively. The data sample corresponds to an integrated luminosity of 2.8 fb^{-1} accumulated with the D0 detector at the Fermilab Tevatron collider.

Flavor Physics and CP Violation - FPCP 2010
May 25-29, 2010
Turin, Italy

[*]Speaker.
[†]for the DØ Collaborations

PoS(FPCP 2010)013

1. Introduction

In the standard model (SM), the light (L) and heavy (H) mass eigenstates of the mixed B_s^0 system are expected to have sizeable mass and decay width differences: $\Delta M_s \equiv M_H - M_L$ and $\Delta\Gamma_s \equiv \Gamma_L - \Gamma_H$. The two mass eigenstates are expected to be almost pure *CP* eigenstates. The *CP*-violating phase that appears in $b \to c\bar{c}s$ decays, due to the interference of the decay with and without mixing, is predicted [1] to be $\phi_s^{J/\psi\phi} = -2\beta_s = 2\arg[-V_{tb}V_{ts}^*/V_{cb}V_{cs}^*] = -0.038 \pm 0.002$, where V_{ij} are elements of the Cabibbo-Kobayashi-Maskawa quark-mixing matrix [2]. New phenomena may alter the observed phase [3] to $\phi_s^{J/\psi\phi} \equiv -2\beta_s + \phi_s^{\Delta}$.

In Ref. [4], we presented an analysis of the decay chain $B_s^0 \to J/\psi\phi$, $J/\psi \to \mu^+\mu^-$, $\phi \to K^+K^-$ based on 1.1 fb^{-1} of data collected with the D0 detector [5] at the Fermilab Tevatron collider. In that analysis we measured $\Delta\Gamma_s$ and the average lifetime of the B_s^0 system, $\overline{\tau}_s = 1/\overline{\Gamma}_s$, where $\overline{\Gamma}_s \equiv (\Gamma_H + \Gamma_L)/2$. The *CP*-violating phase $\phi_s^{J/\psi\phi}$ was also extracted for the first time. The measurement correlated two solutions for $\phi_s^{J/\psi\phi}$ with two corresponding solutions for $\Delta\Gamma_s$. Improved precision was obtained by refitting the results using additional experimental constraints [6]. Here we review D0 results of an analysis that includes information on the B_s^0 flavor at production time. Adding this information resolves the sign ambiguity on $\phi_s^{J/\psi\phi}$ for a given $\Delta\Gamma_s$ and improves the precision of the measurement. The D0 result include measurement of $\Delta\Gamma_s$, the average lifetime of the B_s^0 system, $\overline{\tau}_s = 1/\overline{\Gamma}_s$, where $\overline{\Gamma}_s \equiv (\Gamma_H + \Gamma_L)/2$, and the *CP*-violating phase $\phi_s^{J/\psi\phi}$. The data sample corresponds to an integrated luminosity of 2.8 fb^{-1} collected with the D0 detector [5] at the Fermilab Tevatron collider.

2. Data Selection and Reconstruction

The work reviewd in this paper is based on data accumulated by the D0 detector [5] between October 2002 and June 2007. We reconstruct the decay chain $B_s^0 \to J/\psi\phi$, $J/\psi \to \mu^+\mu^-$, $\phi \to K^+K^-$ from candidate $(J/\psi, \phi)$ pairs consistent with coming from a common vertex and having an invariant mass in the range 5.0 – 5.8 GeV. The event selection follows that in Ref. [4]. The invariant mass distribution of the 48047 candidates is shown in Fig. 1. The curves are projections of the maximum likelihood fit, described below. The fit assigns 1967±65 (stat) events to the B_s^0 decay. The flavor of the initial state of the B_s^0 candidate is determined by exploiting the properties of particles produced by the other b hadron ("opposite-side tagging") and the properties of particles accompanying the B_s^0 meson ("same-side tagging"). The variables used to construct the opposite-side tagging are described in Ref. [7]. The only difference to the description in Ref. [7] is that the events that do not contain either the opposite lepton or the secondary vertex, and that were not used for the flavor tagging before, are now tagged with the event-charge variable defined in Ref. [7].

3. Flavor Tagging

Flavor tagging includes both opposite side tagging (OST) and same side tagging (SST) methods. The OST discriminators are based primarily on the presence of a muon or an electron from the decay of the other B hadron produced in the $p\overline{p}$ interaction. If a charged lepton is not found, the algorithm attempts to reconstruct the decay vertex of the opposite-side B hadron and determine the net charge of tracks forming the vertex.

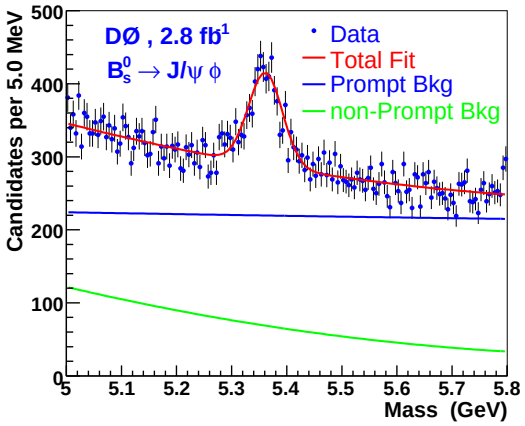

Figure 1: The invariant mass distribution of the $(J/\psi,\phi)$ system for B_s^0 candidates. The curves are projections of the maximum likelihood fit (see text).

The SST is based on the sign of an associated charged kaon formed in the hadronization process. A B_s^0 $(\bar{b}s)$ meson is expected to be accompanied by a strange meson, e.g. K^+ $(u\bar{s})$ meson that can be used for flavor tagging. Such a configuration is formed when the initial $\bar{b}$ antiquark picks up an s quark from a virtual $s\bar{s}$ pair and the $\bar{s}$ antiquark becomes a constituent of an accompanying K^+ meson. Candidates for the associated kaon are all charged tracks with transverse momentum $p_T > 500$ MeV that are not used in the B_s^0 reconstruction. We define the quantity $\Delta R = \sqrt{(\Delta\phi)^2 + (\Delta\eta)^2}$, where $\Delta\phi$ $(\Delta\eta)$ is the distance in the azimuthal angle (pseudorapidity) between the given track and the B_s meson, and select the track with the minimum value of ΔR. The corresponding discriminating variable for the flavor tagging is defined as the product of the particle charge and ΔR. Another discriminating variable is $Q_{\rm jet}$, the p_T-weighted average of all track charges q_i within the cone $\cos[\angle(\vec{p},\vec{p}_B)] > 0.8$ around the B meson: $Q_{\rm jet} = [\sum_i q^i (p_T^i)^{0.6}]/\sum_i (p_T^i)^{0.6}$.

The discriminating variables of both the same-side and opposite-side tagging are combined using the likelihood-ratio method described in Ref. [7]. A tag is defined for 99.7% of events. The performance of the combined tagging is taken from a Monte Carlo(MC) simulation of the $B_s^0 \to J/\psi\phi$ process and is verified with the $B^\pm \to J/\psi K^\pm$ process for which we find the simulated tagging to be in agreement with data. The effective tagging power, as defined in Ref [7], is $\mathscr{P} = (4.68 \pm 0.54)\%$. It is a significant improvement over the performance of the opposite-side tagging alone, $\mathscr{P} = (2.48 \pm 0.22)\%$ [7]. The purity of the flavor tag as a function of an over-all flavor discriminant is determined and parametrized, and the related probability P(B_s) of having a pure state B_s^0 at $t = 0$ is used event-by-event in the fit described below.

4. Maximum likelihood fit

An unbinned maximum likelihood fit was performed to the proper decay time, three decay angles characterizing the final state, and mass of the B_s^0 candidate. The likelihood function $\mathscr{L}$ is given by:

$$\mathscr{L} = \prod_{i=1}^{N} [f_{sig}\mathscr{F}_{sig}^i + (1 - f_{sig})\mathscr{F}_{bck}^i], \tag{4.1}$$

where N is the total number of events, and f_{sig} is the fraction of signal in the sample. The function $\mathscr{F}^i_{sig}$ describes the distribution of the signal in mass, proper decay time, and the decay angles. For the signal mass distribution, we use a Gaussian function with free mean and width. The proper decay time distribution of the L or H component of the signal is parametrized by an exponential convoluted with a Gaussian function. The width of the Gaussian is taken from the event-by-event estimate of the ct uncertainty $\sigma(ct)$, scaled by an overall calibration factor determined from the fit to the prompt component of the background. $\mathscr{F}^i_{bck}$ is the product of the background mass, proper decay time, and angular probability density functions. Background is divided into two categories. "Prompt" background is due to directly produced J/ψ mesons accompanied by random tracks arising from hadronization. This background is distinguished from "non-prompt" background, where the J/ψ meson is a product of a B-hadron decay while the tracks forming the ϕ candidate emanate from a multibody decay of a B hadron or from hadronization.

The decay amplitude of the B_s^0 and $\overline{B}_s^0$ mesons is decomposed into three independent components corresponding to linear polarization states of the vector mesons J/ψ and ϕ, which are either longitudinal (0) or transverse to their direction of motion, and parallel ($\|$) or perpendicular ($\perp$) to each other. The time evolution of the angular distribution of the decay products, expressed in terms of the magnitudes $|A_0|$, $|A_\||$, and $|A_\perp|$, and two relative strong phases $\delta_1 = -\delta_\| + \delta_\perp$ and $\delta_2 = -\delta_0 + \delta_\perp$ of the amplitudes, is given in Ref. [8]:

$$\begin{aligned}
&\frac{d^4\Gamma}{dt\,d\cos\theta\,d\varphi\,d\cos\psi} \propto \\
&\quad 2\cos^2\psi(1-\sin^2\theta\cos^2\varphi)|A_0(t)|^2 \\
&\quad +\sin^2\psi(1-\sin^2\theta\sin^2\varphi)|A_\|(t)|^2 \\
&\quad +\sin^2\psi\sin^2\theta|A_\perp(t)|^2 \\
&\quad +(1/\sqrt{2})\sin 2\psi\sin^2\theta\sin 2\varphi\,\mathrm{Re}(A_0^*(t)A_\|(t)) \\
&\quad +\ (1/\sqrt{2})\sin 2\psi\sin 2\theta\cos\varphi\,\mathrm{Im}(A_0^*(t)A_\perp(t)) \\
&\quad -\ \sin^2\psi\sin 2\theta\sin\varphi\,\mathrm{Im}(A_\|^*(t)A_\perp(t)).
\end{aligned} \tag{4.2}$$

Polarization amplitudes for B_s^0 (upper sign) and $\overline{B}_s^0$ (lower sign) are given by the following equations:

$$\begin{aligned}
|A_{0,\|}(t)|^2 &= |A_{0,\|}(0)|^2\left[\mathscr{T}_+ \pm e^{-\overline{\Gamma}t}\sin\phi_s\ \sin(\Delta M_s t)\right], \\
|A_\perp(t)|^2 &= |A_\perp(0)|^2\left[\mathscr{T}_- \mp e^{-\overline{\Gamma}t}\sin\phi_s\ \sin(\Delta M_s t)\right],
\end{aligned}$$

$$\begin{aligned}
\mathrm{Re}(A_0^*(t)A_\|(t)) &= |A_0(0)||A_\|(0)|\cos(\delta_2-\delta_1) \\
&\times\left[\mathscr{T}_+ \pm e^{-\overline{\Gamma}t}\sin\phi_s\ \sin(\Delta M_s t)\right],
\end{aligned}$$

$$\begin{aligned}
\mathrm{Im}(A_0^*(t)A_\perp(t)) &= |A_0(0)||A_\perp(0)|| \\
&\times[e^{-\overline{\Gamma}t}(\pm\sin\delta_2\cos(\Delta M_s t) \mp \cos\delta_2\sin(\Delta M_s t)\cos\phi_s) - \\
&(1/2)(e^{-\Gamma_H t}-e^{-\Gamma_L t})\sin\phi_s\ \cos\delta_2],
\end{aligned}$$

$$\begin{aligned}\mathrm{Im}(A_\parallel^*(t)A_\perp(t)) &= |A_\parallel(0)||A_\perp(0)| \\ &\times[\, e^{-\overline{\Gamma}t}(\,\pm\sin\delta_1\cos(\Delta M_s t)\mp\cos\delta_1\sin(\Delta M_s t)\cos\phi_s) \\ &-(1/2)(e^{-\Gamma_H t}-e^{-\Gamma_L t})\sin\phi_s\ \cos\delta_1],\end{aligned}$$

where $\mathscr{T}_\pm = (1/2)\left[(1\pm\cos\phi_s)e^{-\Gamma_L t}+(1\mp\cos\phi_s)e^{-\Gamma_H t}\right]$. For a given event, the decay rate is the sum of the B_s^0 and $\overline{B}_s^0$ rates weighted by $\mathrm{P}(B_s)$ and $1-\mathrm{P}(B_s)$, respectively, and by the detector acceptance.

In the coordinate system of the J/ψ rest frame (where the ϕ meson moves in the x direction, the z axis is perpendicular to the decay plane of $\phi\to K^+K^-$, and $p_y(K^+)\geq 0$), the transversity polar and azimuthal angles (θ,φ) describe the direction of the μ^+, and ψ is the angle between $\vec{p}(K^+)$ and $-\vec{p}(J/\psi)$ in the ϕ rest frame.

The acceptance and resolution of the three angles were modeled by fits using polynomial functions, with parameters determined using MC simulations. Events generated uniformly in the three-angle space were processed through the standard GEANT-based [9] simulation of the D0 detector, and reconstructed and selected as real data. Simulated events were reweighted to match the kinematic distributions observed in the data.

The proper decay time distribution shape of the background is described as a sum of a prompt component, modeled as a Gaussian function centered at zero, and a non-prompt component. The non-prompt component is modeled as a superposition of one exponential for $t<0$ and two exponentials for $t>0$, with free slopes and normalizations. The distributions of the backgrounds in mass, $\cos\theta$, φ, and $\cos\psi$ are parametrized by low-order polynomials. We also allow for a background term analogous to the interference term of the A_0 and $A_\parallel$ waves, with one free coefficient. For each of the above background functions we use two separate sets of parameters for the prompt and non-prompt components.

"Prompt" background is due to directly produced J/ψ mesons accompanied by random tracks arising from hadronization. This background is distinguished from "non-prompt" background, where the J/ψ meson is a product of a B-hadron decay while the tracks forming the ϕ candidate emanate from a multibody decay of a B hadron or from hadronization. Each component of $\mathscr{F}^i_{bck}$ is a product of the corresponding mass, proper decay time and angular function. The signal and background parametrization is described below. There are 33 free parameters in the fit.

The high degree of correlation between ΔM_s, ϕ_s, and the two CP-conserving strong phases δ_1 and δ_2 makes it difficult to obtain stable fits when all of them are allowed to vary freely. In the following, we fix ΔM_s to 17.77 ± 0.12 ps^{-1}, as measured in Ref. [10]. The phases analogous to δ_i have been measured for the decay $B_d^0\to J/\psi K^*$ at the B factories. We allow the phases δ_i to vary around the the world-average values [11] for the $B_d^0\to J/\psi K^*$ decay, $\delta_1=-0.46$ and $\delta_2=2.92$, under a Gaussian constraint. The width of the Gaussian, chosen to be $\pi/5$, allows for some degree of violation of the $SU(3)$ symmetry relating the two decay processes, while still effectively constraining the signs of $\cos\delta_i$ to agree with those of Ref. [11]. The mirror solution with $\cos\delta_1<0$ is disfavored on theoretical [12] and experimental [13] grounds.

5. Fit Results

Table 1: Summary of the likelihood fit results for three cases: free ϕ_s, ϕ_s constrained to the SM value, and $\Delta\Gamma_s$ constrained by the expected relation $\Delta\Gamma_s^{SM} \cdot |\cos(\phi_s)|$.

	free ϕ_s	$\phi_s \equiv \phi_s^{SM}$	$\Delta\Gamma_s^{th}$
$\overline{\tau}_s$ (ps)	1.52±0.06	1.53±0.06	1.49±0.05
$\Delta\Gamma_s$ (ps^{-1})	0.19±0.07	0.14±0.07	0.083 ± 0.018
$A_\perp(0)$	0.41±0.04	0.44±0.04	0.45±0.03
$\lvert A_0(0)\rvert^2 - \lvert A_\parallel(0)\rvert^2$	0.34±0.05	0.35±0.04	0.33±0.04
δ_1	−0.52±0.42	−0.48±0.45	−0.47±0.42
δ_2	3.17±0.39	3.19±0.43	3.21±0.40
ϕ_s	$-0.57^{+0.24}_{-0.30}$	$\equiv -0.04$	-0.46 ± 0.28
ΔM_s (ps^{-1})	$\equiv 17.77$	$\equiv 17.77$	$\equiv 17.77$

Results of the fit are presented in Table 1. The fit yields a likelihood maximum at $\phi_s = -0.57^{+0.24}_{-0.30}$ and $\Delta\Gamma_s = 0.19 \pm 0.07$ ps^{-1}, where the errors are statistical only. As a result of the constraints on the phases δ_i, the second maximum, at $\phi_s = 2.92^{+0.30}_{-0.24}$, $\Delta\Gamma_s = -0.19 \pm 0.07$ ps^{-1}, is disfavored by a likelihood ratio of 1:29. Without the constraints on δ_i, ϕ_s shifts by only 0.02 for the $\Delta\Gamma_s > 0$ solution. Confidence level contours in the $\phi_s - \Delta\Gamma_s$ plane, and likelihood profiles as a function of ϕ_s and as a function of $\Delta\Gamma_s$ are shown in Fig. 2. Studies using pseudo-experiments with similar statistical sensitivity indicate no significant biases and show that the magnitudes of the statistical uncertainties are consistent with expectations. The mean value of the statistical uncertainty in ϕ_s from an ensemble generated with the same parameters as obtained in this analysis is 0.33. The test finds allowed ranges at the 90% C.L. of $-1.20 < \phi_s < 0.06$ and $0.06 < \Delta\Gamma_s < 0.30$ ps^{-1}. To quantify the level of agreement with the SM, we use pseudo-experiments with the "true" value of the parameter ϕ_s set to -0.04. We find the probability of 6.6% to obtain a fitted value of ϕ_s lower than -0.57.

Setting $\phi_s = -2\beta_s = -0.04$, as predicted by the SM, we obtain $\Delta\Gamma_s = 0.14 \pm 0.07$ ps^{-1}. This is consistent with the theoretical prediction of 0.088 ± 0.017 ps^{-1} [1]. The results for this fit are shown in the second column in Table 1. The non-zero mixing phase is expected to reduce $\Delta\Gamma_s$ by the factor of $|\cos(\phi_s)|$ compared to its SM value $\Delta\Gamma_s^{SM}$ [8]. In the third column of Table 1 we show results of a fit with $\Delta\Gamma_s$ constrained by this expected behavior.

The measurement uncertainties are dominated by the limited statistics. Uncertainty in the acceptance as a function of the transversity angles is small, the largest effect is on $|A_0(0)|^2 - |A_\parallel(0)|^2$. Effects of the imperfect knowledge of the flavor-tagging purity are estimated by varying the flavor purity parametrization within uncertainties. The "interference" term in the background model accounts for the collective effect of various physics processes. However, its presence may be partially due to detector acceptance effects. Therefore, we interpret the difference between fits with and without this term as a contribution to the systematic uncertainty associated with the background

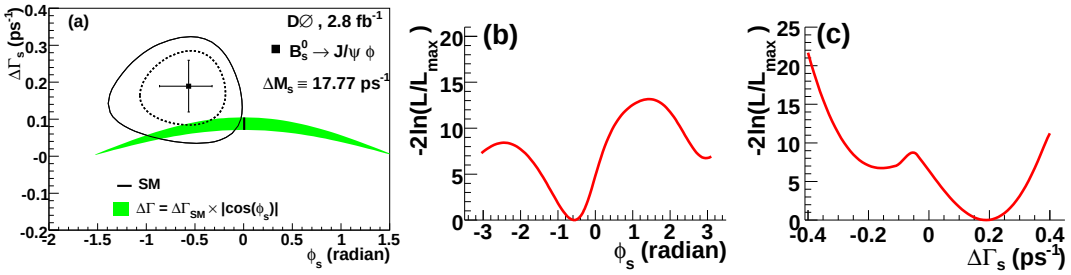

Figure 2: (a) Confidence-level contours in the $\Delta\Gamma_s$ - ϕ_s plane. The curves correspond to expected C.L.= 68.3% (dashed) and 90% (solid). The cross shows the best fit point and one-dimensional uncertainties. Also shown is the SM prediction, $\phi_s = -2\beta_s = -0.04$, $\Delta\Gamma_s = 0.088 \pm 0.017$ ps^{-1} [1]. (b) Likelihood profile of ϕ_s, (c) likelihood profile of $\Delta\Gamma_s$.

model. The main contributions to system atic uncertainties for the case of free ϕ_s are listed in Table 2.

Table 2: Sources of systematic uncertainty in the results for the case of free ϕ_s.

Source	$\overline{\tau}_s$ (ps)	$\Delta\Gamma_s$ (ps^{-1})	$A_\perp(0)$	$\lvert A_0(0)\rvert^2 - \lvert A_\parallel(0)\rvert^2$	ϕ_s
Acceptance	± 0.003	± 0.003	± 0.005	± 0.03	± 0.005
Signal mass model	-0.01	$+0.006$	-0.003	-0.001	-0.006
Flavor purity estimate	± 0.001	± 0.001	± 0.001	± 0.001	± 0.01
Background model	$+0.003$	$+0.02$	-0.02	-0.01	$+0.02$
ΔM_s input	± 0.01	± 0.001	± 0.001	± 0.001	$+0.06, -0.01$
Total	± 0.01	$+0.02, -0.01$	$+0.01, -0.02$	± 0.03	$+0.07, -0.02$

6. Conclusions

In summary, from a fit to the time-dependent angular distribution of the flavor-tagged decays $B_s^0 \to J/\psi\phi$, D0 measured the average lifetime of the $(B_s^0,\ \overline{B}_s^0)$ system, $\overline{\tau}(B_s^0) = 1.52 \pm 0.05 \pm 0.01$ ps, the width difference between the light and heavy B_s^0 eigenstates, $\Delta\Gamma_s = 0.19 \pm 0.07(\text{stat})^{+0.02}_{-0.01}(\text{syst})$ ps^{-1}, and the *CP*-violating phase, $\phi_s = -0.57^{+0.24}_{-0.30}(\text{stat})^{+0.07}_{-0.02}(\text{syst})$. D0 also measure the magnitude of the decay amplitudes. In the fits, we set the oscillation frequency to $\Delta M_s = 17.77$ ps^{-1}, as measured in Ref. [10], and we impose a Gaussian constraint with a width of $\pi/5$ to the deviation of the strong phases from the values $\delta_1 = -0.46$ and $\delta_2 = 2.92$ of Ref. [11]. The allowed 90% C.L. intervals of $\Delta\Gamma_s$ and of ϕ_s are $0.06 < \Delta\Gamma_s < 0.30$ ps^{-1} and $-1.20 < \phi_s < 0.06$. The SM hypothesis for ϕ_s has a *P*-value of 6.6%.

Above results supersede the previous D0 measurements [4] that were based on the untagged decay $B_s^0 \to J/\psi\phi$ and a smaller data sample. The D0 results are consistent with the CDF results [14] based on same luminosity of data.

References

[1] A. Lenz, and U. Nierste, J. High Energy Physics **0706**, 072 (2007).

[2] M. Kobayashi and T. Maskawa, Prog. Theor. Phys. **49**, 652 (1973).

[3] M. Bona *et al.*, J. High Energy Physics **0610**, 081 (2006).

[4] D0 Collaboration, V. M. Abazov *et al.*, Phys. Rev. Lett. **98**, 121801 (2007).

[5] D0 Collaboration, V. M. Abazov *et al.*, Nucl. Instrum. Methods Phys. Res. A **565**, 463 (2006).

[6] D0 Collaboration, V. M. Abazov *et al.*, Phys. Rev. D **76**, 057101 (2007).

[7] D0 Collaboration, V. M. Abazov *et al.*, Phys. Rev. D **74**, 112002 (2006).

[8] I. Dunietz, R. Fleischer, and U. Nierste, Phys. Rev. D **63**, 114015 (2001).

[9] R. Brun and F. Carminati, CERN Program Library Long Writeup W5013, 1993 (unpublished).

[10] CDF Collaboration, A. Abulencia *et al.*, Phys. Rev. Lett. **97**, 242003 (2006).

[11] C. Amsler *et al*. (Particle Data Group), PL B667, 1 (2008) and 2009 partial update for the 2010 edition (URL: http://pdg.lbl.gov).

[12] M. Suzuki, Phys. Rev. D **64**, 117503 (2001).

[13] BaBar Collaboration, B. Aubert *et al.*, arXiv:0704.0522[hep-ex].

[14] CDF Collaboration, T. Aaltonen *et al.*, CDF Public Note CDF/ANAL/BOTTOM/PUBLIC/9458, (2008).